JOURNAL OF MATERIALS SCIENCE 22 (1987) 3463–3469

On lateral cracks in glass

SREERAM SRINIVASAN, R. O. SCATTERGOOD
Department of Materials Engineering, North Carolina State University, Box 7907, Raleigh, North Carolina 27695-7907, USA

The importance of lateral cracks in solid particle erosion of brittle materials has been confirmed as a result of a large number of previous investigations in this area. Even though the underlying mechanism of steady-state erosion of a brittle material is the formation and growth of lateral cracks, the surface morphology of the eroded material does not readily indicate this aspect. This has precipitated the need for a study of single impact events. This study concentrates on lateral cracks in glass produced by solid particle impacts. Single impacts are studied in terms of lateral crack extensions and their probability of chipping at two angles of impact of 20 and 90°. Comparisons between these two sets of data were made at the same normal component of velocity to clearly bring out behavioural differences at the two angles of impact. Steady-state erosion results are then interpreted in terms of the above results obtained from a study of single impacts. There appears to be marked agreement between these results and experimental observations. The same trend was observed in strength degradation measurements. Increased chipping and lateral crack extensions in the 20° impact situation has been explained in terms of linear elastic fracture mechanics, as opposed to the plastic deformation mechanism proposed earlier. The importance of single impacts in the study of steady-state erosion of brittle materials by solid particle impact is well demonstrated by this study.

1. Introduction

It is now well established that material removal by solid particle erosion in brittle materials occurs by the formation and growth of lateral cracks, finally resulting in chipping. Even though steady-state erosion of brittle materials has been well documented, the mechanism of erosion has only been generally stated. Models of dynamic and quasi-static impacts due to Evans *et al.* [1] and Wiederhorn and Lawn [2] do not offer completely comprehensive explanations. Knowing that lateral fractures from adjacent impacts show little interaction [1] and pursuing the idea that, to a first approximation, the material removal can be considered a summation of single-impact removal events, the need to study single impacts emerges. The angle of incidence of the impacting particle has been shown to affect the erosion rate in brittle materials in most of the earlier work on brittle materials. Investigations on brittle materials so far have noticed increased erosion at low angles of impact in the range of 15 to 30°. This was explained in terms of plastic deformation and an increased tendency of the brittle material towards ductile behaviour. The purpose of this work was to closely observe the single impact events on commercial glass specimens at various particle velocities and angles of impact. The probability of chip removal was determined. A chip is removed if a lateral crack deflects upward and intersects the surface. If the lateral crack remains below the surface, no chip is removed. The work also examines the velocity dependence of lateral crack extensions, the need for which has been stressed by Evans [3]. These observations were used to draw comparisons between normal and low-angle impact conditions at the same normal component of particle velocity.

2. Experimental details

2.1. Material

Glass specimens were cut to size of 28 mm × 32 mm × 2 mm from a window-plane glass that is commercially available. The glass was used in the as-received condition without any further surface preparation.

2.2. Apparatus and procedure

The specimens were impacted using an erosion set-up described earlier [4] using 80 grit Norton E17 alundum particles of mean size 270 μm that were accelerated with an air blast. This was done in a controlled way so as to obtain single impacts, using a plate with a slot which acted as a shutter to limit the total number of impacts. For the particles to impact the specimen the slot was aligned with the nozzle and the specimen for a short time. The same set-up was used for normal impacts at velocities of 30, 39, 55, 70 m sec^{-1} and for 20° oblique impacts at 55 and 70 m sec^{-1}.

The impacts were then studied under an Olympus optical microscope using reflected polarized light. This clearly delineated the impacts for which the lateral cracks had reached the surface and for the ones that had not, by observing the fringe pattern caused by stress concentration at the crack tip and the wedge between the two faces of the lateral crack. Counts of impacts for which the chips were still attached and those for which chips had been removed were made for each specimen. Care was exercised to generate a sufficiently large number of impacts for the results to

0022–2461/87 $03.00 + .12

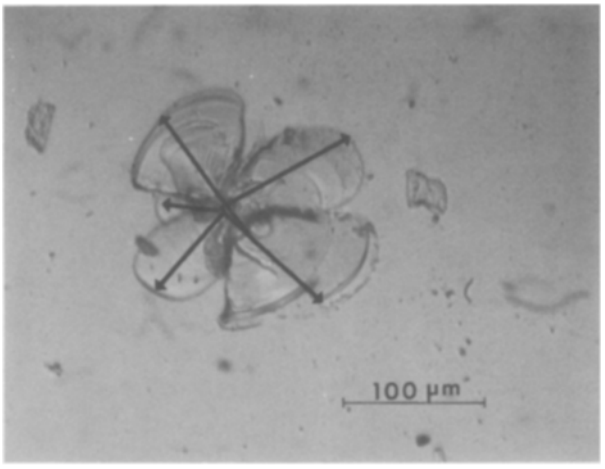

Figure 1 Shows the method of crack extension measurement. Arrows indicate the directions in which counts have been made.

possess statistical significance. The probabilities of removal events and non-removal events were then calculated as fractions of the total number of impacts.

Lateral crack extensions in single impacts occur in all directions. For this reason, extension measurements as defined by Evans [3] must be made in all directions as shown in Fig. 1, and a mean extension for that impact must be calculated. The eyepiece scale of the microscope was used to measure lateral crack extensions in all the directions of crack extension and an average extension for that impact was calculated. On each specimen such average extensions were determined on 20 to 25 single impacts, and the mean lateral crack extension for that specimen was obtained as an arithmetic mean of the average extensions. Four specimens were thus investigated for each velocity and angle of incidence.

3. Results

3.1. Probability measurements

Chipped single impacts obtained in the statistical counts were used in combination with the total number of impacts on the specimen to calculate the removal or chipping probability for each impact velocity and angle condition. Table I shows the statistical counts and the calculated probabilities on specimens impacted at 55 m sec^{-1} at 90 and 20°.

Fig. 2 shows the velocity dependence of chipping or removal probability. The chipping probability has been plotted against the normal component of velocity for the case of normal and oblique impact condition at various velocities. A linear least-squares fit has been drawn through the data for each of the two impact conditions. This has been done to aid comparison of the data for the two conditions of impact. An upward displacement of the oblique impact data as compared to the normal impact can be noticed.

Fig. 2 also shows a velocity threshold below which the chipping probability is zero. The velocity threshold for 90° impact, obtained by extrapolation of the straight line to zero chipping probability, was approximately 12 m sec^{-1}. Experiments at velocities close to 12 m sec^{-1} for the 90° impact condition confirmed that chip removal was negligible even though noticeable lateral cracking occurred. The limited data for 20° impact make it difficult to obtain a threshold value, but it appears to be close to zero velocity as seen from Fig. 2.

3.2. Lateral crack extensions

As discussed in Section 2.2, lateral crack extensions of the single impact were measured using the eyepiece scale at 220× magnification and converted to true extensions in millimetres by a conversion factor. Table II gives the counts made on 22 such single impacts on a specimen impacted at 55 m sec^{-1} at 90°. The average crack extension per impact was used to calculate a mean lateral crack extension for that specimen. For each impact velocity and impact angle, mean lateral crack extensions were calculated on four different specimens. Mean lateral crack extensions for various specimens and conditions have been shown in Table III. Standard deviations for each of these measurements have also been indicated. The scatter is found to be within reasonable limits considering the statistical method that has been used to measure the extensions.

Log (mean lateral crack extension) against log (normal component of velocity) has been plotted in Fig. 3 to show the velocity dependence of lateral crack extensions. The lateral crack extension data used in this plot approximate the scatter in the results. The plots are based on data obtained for normal and 20° impacts at the respective velocities. A linear least-squares fit through the data has been drawn for each of the impact conditions. The fit through normal impact

TABLE I Statistical counts of single impact events on glass (particle size = 270 μm).

Unattached	Attached	Total impacts	Probability	
			Removal	Non-removal
Normal impact at 55 m sec^{-1}				
837	434	1271	0.659	0.341
728	343	1071	0.680	0.320
697	460	1157	0.602	0.398
855	394	1249	0.685	0.315
1021	457	1478	0.691	0.309
Oblique impact at 55 m sec^{-1}				
545	1562	2107	0.259	0.741
532	1260	1792	0.297	0.703
629	1746	2375	0.265	0.735
615	1822	2437	0.252	0.748

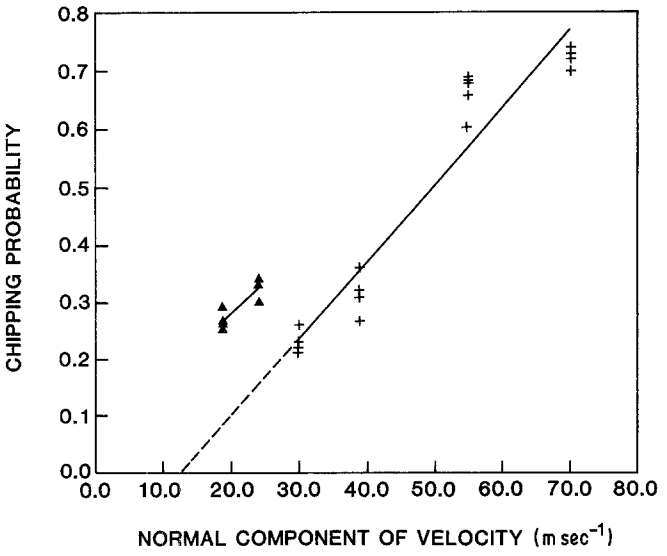

Figure 2 Chipping probability dependence on normal velocity component: (+) normal impact, (▲) oblique impact at 20°.

data follows a power-law relationship between normal velocity component and the mean lateral crack extension such as

$$c \propto V^n$$

where V is the normal component of impact velocity, c is the mean lateral crack extension and the exponent n is found to be 0.770.

An upward displacement of the data for impact at 20° occurs relative to the normal impact data as shown in Fig. 3. This in effect means that at the same normal component of velocity, 20° impact produces a larger lateral crack extension. This is seen by comparing the extrapolated (dashed line) values for normal impact with those for 20° impact. A similar difference for chipping probability is evident from Fig. 2.

3.3. Optical micrographs

The micrographs reveal that chipping occurs by the initiation and growth of lateral cracks in all directions from the impact zone and their subsequent intersection with the surface. No preferential extension of lateral cracks in any direction has been noticed in oblique incidence as is evident from Fig. 4. Neither was there any evidence by plastic furrowing or cutting in the zone surrounded by lateral cracks as seen by Hockey *et al.* [5] on SiC, where material removal occurs by plastic scooping or scratching-type events. This does not mean that there was an absence of a deformed zone under the point of indentation, which comes from the removal of the singularity of stresses at that point. Deformation occurs in the zone due to plastic flow or viscous flow, depending on the material [6].

Fig. 5 shows a removal event where intersections of lateral cracks with the free surface have led to stress relief. This is evident by the absence of a fringe pattern. Fringes would be observed if there were stress concentrations in the material being observed, as the observations were made using a reflected polarized

TABLE II Statistical counts of lateral crack extensions (55 m sec^{-1} normal impact)

Lateral	Crack	Extension	Counts*	(110 divisions = 0.5 mm)	Average size*
32	26	21	15	18	0.10
16	20	22	–	–	0.09
20	18	20	–	–	0.09
20	17	16	–	–	0.08
16	18	16	–	–	0.08
17	17	12	11	–	0.06
18	20	–	–	–	0.09
30	12	20	16	–	0.09
15	28	14	–	–	0.09
16	16	10	–	–	0.06
24	13	11	–	–	0.07
11	15	11	–	–	0.06
23	20	17	19	–	0.09
17	15	–	–	–	0.07
12	20	9	–	–	0.06
20	18	14	–	–	0.08
32	24	–	–	–	0.13
8	10	–	–	–	0.04
12	6	–	–	–	0.04
10	9	8	–	–	0.04
17	10	–	–	–	0.06
8	9	11	16	–	0.05

*Mean lateral crack extension = 0.073 mm

TABLE III Lateral crack extensions (mm)

Normal impact at 30 m sec^{-1}	Standard deviation	Normal impact at 39 m sec^{-1}	Standard deviation	Normal impact at 55 m sec^{-1}	Standard deviation	Normal impact at 70 m sec^{-1}	Standard deviation	Oblique impact at 55 m sec^{-1}	Standard deviation	Oblique impact at 70 m sec^{-1}	Standard deviation
0.039	±0.01	0.043	±0.01	0.073	±0.021	0.080	±0.022	0.036	±0.011	0.043	±0.012
0.042	±0.008	0.047	±0.009	0.064	±0.012	0.070	±0.018	0.040	±0.008	0.044	±0.010
0.045	±0.008	0.049	±0.01	0.061	±0.020	0.079	±0.027	0.039	±0.009	0.045	±0.009
0.045	±0.008	0.045	±0.009	0.066	±0.013	0.079	±0.021	0.040	±0.007	0.047	±0.014

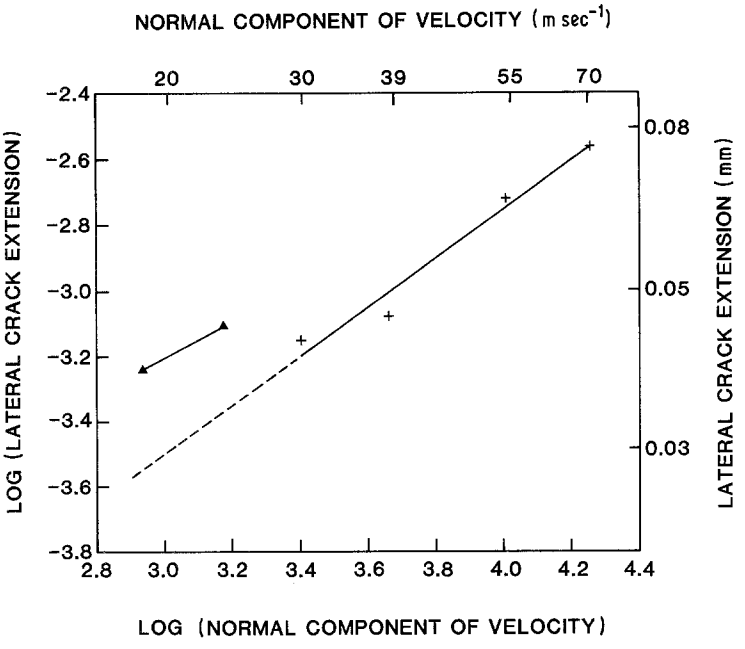

Figure 3 Log–log plot showing velocity dependence of lateral crack extension: (+) normal impact, (▲) oblique impact at 20°.

light. A non-removal event, where a lateral crack has not yet intersected with the surface, is shown in Fig. 6. Fringes reveal a stress concentration at the tip.

Figs 7 and 8 show the variation of lateral crack extension with velocity of impact.

Fig. 9 shows the impacting particles used in the study. The figure shows their angular morphology. A discussion on particle shapes appears in the study by Shin *et al.* [7].

4. Discussion

Fig. 2 indicates a linear dependence of chipping probability on the normal component of velocity. An increase in probability for oblique incidence as compared to normal incidence is indicated. Assuming that erosion rates will scale with chipping probability, this suggests that oblique incidence is more erosive than normal incidence at the same normal velocity component for this study of single impacts.

A velocity threshold for the chipping probability has also been noticed for the normal impact situation, but the lateral cracks are still seen to develop even though small in size. Its effect would be a velocity threshold for steady-state erosion, but this threshold would be lower when compared to the one for the single-impact situation. This seems to agree with the concept of a velocity threshold for erosion reported by Evans [3]

Fig. 3 shows a power-law relation between mean lateral crack extension and normal component of velocity. On the assumption that the depth of lateral crack formation depends only on the normal component of velocity [3], the same power law when applied to oblique incidence with its normal component of velocity yields a crack extension value which is about 30 to 39% smaller than the experimentally observed value. This suggests that greater extensions could be due to the tangential velocity component, which is quite significant in case of 20° impacts. A cross-plot between lateral crack extension and the chipping probability at a constant normal component of particle velocity shows increased chipping probability for the low-angle impact condition at the same value of lateral crack extension. This rules out the possibility of a simple size effect for chipping probability.

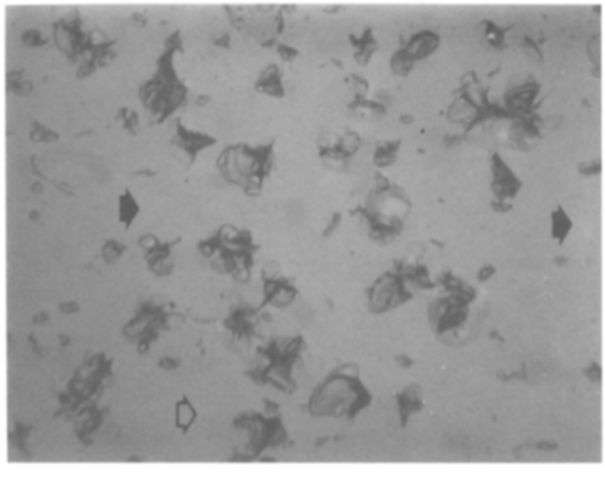

Figure 4 Shows oblique incidence at 55 m sec^{-1} and 20°. Arrow indicates direction of impacting particle motion. × 50.

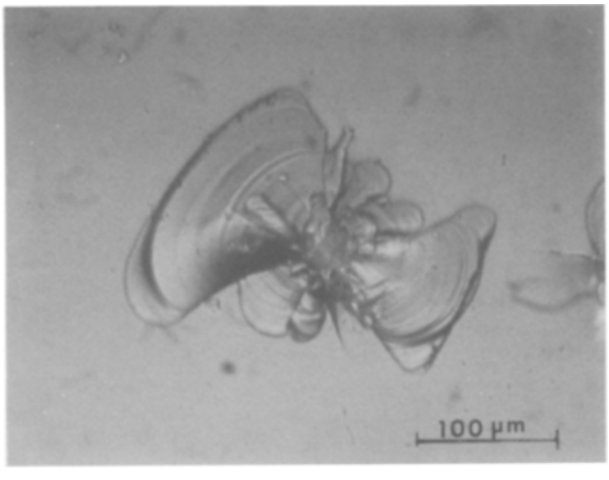

Figure 5 Shows a removal event. Note the absence of interference fringes and plastic furrowing.

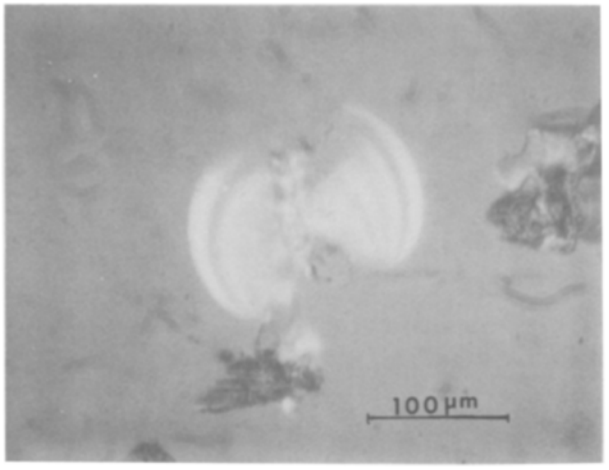

Figure 6 Shows a non-removal event.

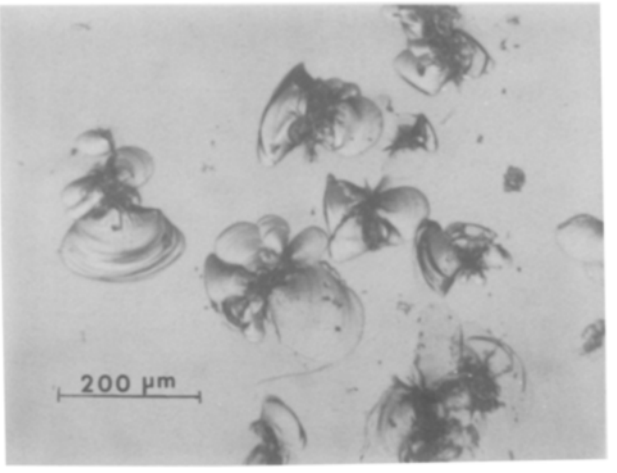

Figure 8 Shows single impact events on specimen impacted at 70 m sec^{-1}, normal incidence.

The net effect of the above observation would then be to increase the erosion efficiency, resulting in an upward displacement of the erosion rate curve for oblique incidence which has in fact been observed in mullite (an equally brittle material) by Morrison *et al.* [8] for the steady-state erosion condition. This lends credence to what has been observed in this work.

The impact angle has been shown to have an effect on the strength degradation of glass. Observations by Wiederhorn *et al.* [6] have shown that the strength degradation predicted by simple velocity resolution is much lower than the observed value at oblique (low angle) impact. This agrees well with the increased lateral crack extension for oblique impact of 20° seen in this study. Assuming, as in earlier studies, that the radial crack sizes are proportional to the lateral crack extensions it is clear that agreement between the two results is not fortuitous. However, the observation regarding preferential lateral crack extension along a certain direction [6] is questionable when compared with the observations of oblique (20°) impacts in this work, as is evident from Fig. 4.

Increased erosion rate values obtained for oblique incidence in many of the earlier works has been attributed to experimental scatter or to plastic deformation [5]. This does not appear convincing in the light of the observations on single impacts in this work.

Particle size has been shown to influence the mechanisms of fracture during solid-particle erosion on brittle materials. The fracture mechanisms can be quasi-static or dynamic. At certain velocities of impact with large particles, materials have shown quasi-static behaviour. This has been inferred from the velocity exponents for erosion rate obtained in those studies [9].

Theoretical analysis of solid-particle impact fracture mechanisms will yield a crack extension against particle velocity relation. There are two basic steps in any such analysis. First, assume that lateral cracks are penny-shaped and subject to point-force tensile loads F at their centre. If K_c is the fracture toughness, the crack extension c is then

$$c \propto (F/K_c)^{2/3} \tag{1}$$

The second step is to relate the net force F, which is due to residual elastic–plastic deformation conditions in the contact zone, to the impacting particle kinematics and in particular the particle velocity. Using the quasi-static analysis for contact conditions given by

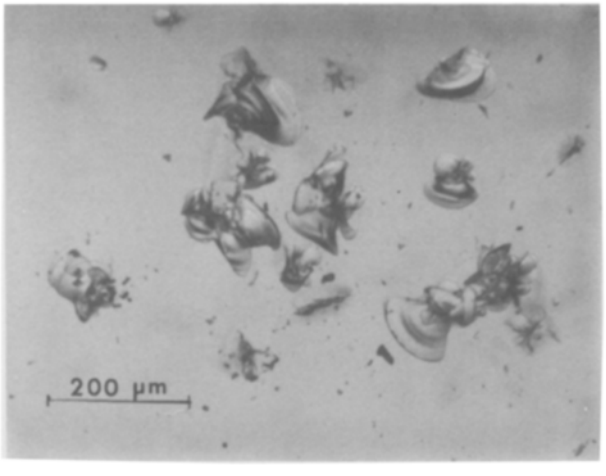

Figure 7 Shows single impact events on specimen impacted at 30 m sec^{-1} normal incidence.

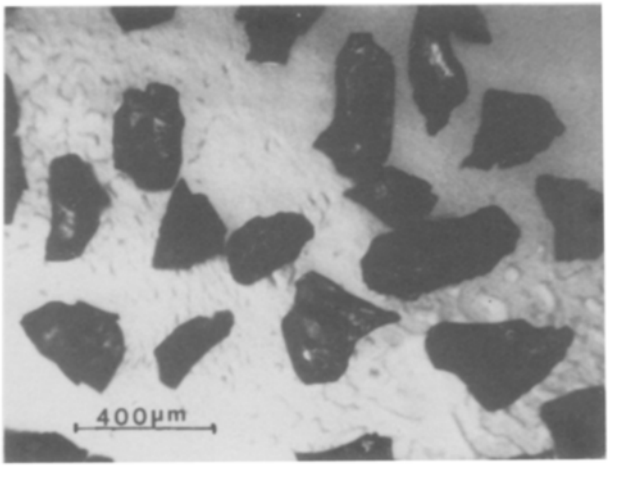

Figure 9 Photomicrograph of the 80 grit Norton E17 aluminium particles showing particle morphology.

Weiderhorn and Lawn [2], it can be shown that

$$\begin{aligned} F &\propto V && \text{for spherical particles} \\ F &\propto V^{4/3} && \text{for wedge-shaped particles} \end{aligned} \quad (2)$$

Combining Equations 1 and 2 gives the quasi-static results

$$\begin{aligned} c &\propto V^{0.66} && \text{for spherical particles} \\ c &\propto V^{0.89} && \text{for wedge-shaped particles} \end{aligned}$$

The measured value of $n = 0.77$ falls between these values, and suggests that the contact conditions can be treated in the quasi-static limit. If one uses the dynamic analysis for contact conditions developed by Evans *et al.* [1], the exponent for spherical particles is determined as 1.33, while that for wedge-shaped particle would be even higher.

Consequently, an assumption that a quasi-static mechanism is operative in the crack extensions obtained in this work appears to be justified. Furthermore, the crack extension dependence on the tangential forces have been shown to be quite significant earlier in the discussion. The same trend has been noticed for chipping probability as well. In the light of the above observations, the assumption by Evans [3] regarding the insensitivity of lateral crack extension to the magnitude of the tangential component of particle velocity for the quasi-static case is questionable.

Residual stresses from the elastic–plastic loading–unloading cycle as suggested by Evans [3] can be assumed to drive the lateral cracks. A penny-shaped crack morphology for the lateral cracks has been assumed as in many of the earlier models. These lateral cracks are seen to propagate in an elastic stress field with primarily a Mode I type of mechanism (penny-shaped crack) for a normal impact situation. For oblique incidence at 20° as in this work, the tangential component becomes significantly large and could lead to a change in stress field distribution causing Mode II or Mode III types of mechanism to operate. This is suggested by the absence of preferential lateral crack extension in any direction at oblique incidence. This would then explain the increased chipping probability and also the increased crack extension in pure LEFM (linear elastic fracture mechanics) terms.

More work on these points is required to corroborate these views and develop a more complete model for the erosion of brittle materials. The observations of this work could form a basis and guide for such a study.

5. Conclusions

The conclusions of the work reported here can be summarized as follows:

1. Comparisons of data on lateral cracks between normal and 20° impact conditions appear to be best when made at the same normal component of particle velocity rather than at the same absolute value.

2. The definite upward shifts in chipping probability and crack extension for oblique single impacts that have been observed would cause an increase in the steady-state erosion as compared to normal incidence at the same normal component of velocity. This has also been observed in steady-state erosion results. Strength degradation results on glass also predict the same trend as regards oblique (low angle) impacts.

3. The measured crack extension of particle velocity fits the simple model for quasi-static contact conditions. Direct observations of crack extension, as done in this work, appears to be the most direct method to test such models. Steady-state erosion results reported in the literature suggest that particle size may affect the contact conditions.

4. With further study, an elastic model using Mode II or Mode III should be developed to explain the observed upward shift. This will aid in developing better models for the solid-particle erosion of brittle materials.

Acknowledgements

The authors gratefully acknowledge the US Department of Energy for support of this work under Grant DE-FG05-84ER45115. The work reported here was done in partial fulfillment of the MS thesis requirement for S. Srinivasan.

References

1. A. G. EVANS, M. E. GULDEN and M. E. ROSENBLATT, *Proc. R. Soc.* **A361** (1978) 343.
2. S. M. WIEDERHORN and B. R. LAWN, *J. Amer. Ceram. Soc.* **62** (1979) 66.
3. A. G. EVANS, "The Science of Ceramic Machining and Surface Finishing," edited by B. J. Hockey and R. W. Rice, NBS Special Publication, 562, Vol. 2 (1979) p. 1.
4. S. K. HOVIS, K. ANAND, H. CONRAD and R. O. SCATTERGOOD, *Wear* **101** (1985) 69.
5. B. J. HOCKEY, S. M. WIEDERHORN and H. JOHNSON, "Fracture Mechanics of Ceramics," Vol. 3 (Plenun, New York, 1978) p. 379.
6. S. M. WIEDERHORN, B. R. LAWN and B. J. HOCKEY, *J. Amer. Ceram. Soc.* **62** (1978) 639.
7. Y. SHIN and H. CONRAD, Progress Report: DOE/ER/45115-1, June 1st 1984 to Jan. 31st 1985, p. 124.
8. C. T. MORRISON, J. L. ROUTBORT and R. O. SCATTERGOOD, *Wear* **105** (1985) 19.
9. R. O. SCATTERGOOD and J. L. ROUTBORT, *J. Amer. Ceram. Soc.* **66** (1983) C-184.

Received 9 June 1986
and accepted 15 January 1987